

Diverse Optical and Photosynthetic Properties in a Neotropical Dry Forest during the Dry Season: Implications for Remote Estimation of Photosynthesis¹

John A. Gamon²

Center for Environmental Analysis (CEA-CREST) & Department of Biological Sciences, California State University, Los Angeles, 5151 State University Drive, Los Angeles, CA 90032 U.S.A.

Kaoru Kitajima, Stephen S. Mulkey

Department of Botany, University of Florida, 220 Bartram Hall, PO Box 118526, Gainesville, FL 32611 U.S.A.

Lydia Serrano

Departament d'Enginyeria Agroalimentària i Biotecnologia, Campus del Baix Llobregat UPC Edifici ESAB – Av. Canal Olímpic, s/n, 08860 Castelldefels, Spain

and

S. Joseph Wright

Smithsonian Tropical Research Institute, Apartado 2072, Balboa, Republic of Panama

ABSTRACT

Using optical and photosynthetic assays from a canopy access crane, we examined the photosynthetic performance of tropical dry forest canopies during the dry season in Parque Metropolitano, Panama City, Panama. Photosynthetic gas exchange, chlorophyll fluorescence, and three indices derived from spectral reflectance (the normalized difference vegetation index, the simple ratio, and the photochemical reflectance index) were used as indicators of structural and physiological components of photosynthetic activity. Considerable interspecific variation was evident in structural and physiological behavior in this forest stand, which included varying degrees of foliage loss, altered leaf orientation, stomatal closure, and photosystem II downregulation. The normalized difference vegetation index and the simple ratio were closely related to canopy structure and absorbed radiation for most species, but failed to capture the widely divergent photosynthetic behavior among evergreen species exhibiting various degrees of downregulation. The photochemical reflectance index and chlorophyll fluorescence were related indicators of photosynthetic downregulation, which was not detectable with the normalized difference vegetation index or simple ratio. These results suggest that remote sensing methods that ignore downregulation cannot capture within-stand variability in actual carbon flux for this diverse forest type. Instead, these findings support a sampling approach that derives photosynthetic fluxes from a consideration of both canopy light absorption (*e.g.*, normalized difference vegetation index) and photosynthetic light-use efficiency (*e.g.*, photochemical reflectance index). Such sampling should improve our understanding of controls on photosynthetic carbon uptake in diverse tropical forest stands.

RESUMEN

Caracterizamos la conducta fotosintética de diversas especies presentes en el dosel de un bosque seco tropical (Parque Metropolitano, Ciudad de Panamá, Panamá) durante la época seca utilizando técnicas ópticas y de intercambio de gases. Se utilizaron como indicadores de los componentes estructurales y fisiológicos de la actividad fotosintética medidas de intercambio de gases y de fluorescencia de la clorofila así como tres índices derivados de análisis de reflectancia espectral: NDVI (índice de vegetación de diferencia normalizada), SR (razón simple) y PRI (índice de reflectancia fotoquímica). En este bosque se evidenció una gran variación interespecifica en la estructura del dosel (pérdida de hojas y cambios en la orientación de las hojas) así como en la conducta fisiológica (diferentes grados de cierre estomático y regulación a la baja del sistema fotosintético II). Los índices NDVI y SR mostraron una estrecha correlación con la estructura de la cubierta del dosel y la radiación absorbida para la mayoría de especies estudiadas, pero se mostraron poco útiles para detectar los cambios en la actividad fotosintética en las especies perennes que presentaban diversos grados de regulación del fotosistema a la baja. La fluorescencia de la clorofila y el índice PRI mostraron una estrecha relación y ambos fueron buenos indicadores de la regulación del fotosistema a la baja en el PSII, mientras que esta conducta no fue detectada por los índices NDVI y SR. Los resultados obtenidos indican que los métodos de teledetección que ignoran la regulación del fotosistema a la baja no consiguen detectar la variabilidad existente en el flujo de CO₂ en este bosque tropical tan diverso.

Key words: APAR; biodiversity; canopy crane; normalized difference vegetation index (NDVI); photosynthetic downregulation; photochemical reflectance index (PRI); radiation-use efficiency; tropical dry forest; xanthophyll cycle.

MANY VEGETATION CLASSIFICATION SCHEMES lump the forests of Central America into one or two vegetation types (*e.g.*, “rainforest” and “seasonal forest,” *e.g.*, Whittaker 1975, Collinson 1988), and some global models of vegetation-atmosphere fluxes consider

tropical forests as a single functional type (*e.g.*, Sellers *et al.* 1996b). Such simplifying assumptions are necessary if vast forest areas are to be included in global-scale climate models, which are only beginning to contain realistic parameterizations of vegetated surface properties.

In contrast, ecological studies of tropical forests have emphasized their species, structural, and functional diversity, all of which

¹ Received 15 October 2004; revision accepted 8 June 2005.

² Corresponding author; e-mail: jgamon@calstatela.edu

contribute to their renowned biodiversity (Gentry 1988). For example, many forests of Central America are complex mixtures of evergreen and drought-deciduous species exhibiting dramatically varying morphological and phenological responses to seasonal drought (Wright 1996). Presumably, this structural diversity of seasonally dry tropical forests is associated with considerable physiological diversity. Recent studies from a Panamanian dry forest have confirmed a diversity of leaf phenology and physiological responses to spatial and temporal environment (Mulkey *et al.* 1996). Both leaf age and light microenvironment within the canopy affect the leaf photosynthetic capacity within each species, and the degree of these responses vary greatly among species (Kitajima *et al.* 1997a, b). These species also differ in rooting depth, stem water storage capacity, and leaf area to sapwood ratio, which jointly determine the ability to maintain water supply and whole-tree transpiration during the dry season (Meinzer *et al.* 1997, 1999). If we are to understand the role of tropical dry forests in larger biogeochemical processes, further studies exploring the physiological and morphological diversity of seasonally dry tropical forests are warranted. In this study, we characterize this diversity for a dry tropical forest site. Using the Smithsonian Institution's Canopy Access Crane (Parker *et al.* 1992), we examined the linked optical, structural, and photosynthetic properties of a variety of dominant forest species in a Panamanian forest during the dry season (February–April, 1994).

An understanding of forest physiology is critical to an understanding of climate, because the photosynthetic and stomatal physiology of vegetation stands can exert significant control over vegetation-atmosphere fluxes, and consequently on climate (Shukla *et al.* 1990, Sellers *et al.* 1996a). Many tropical forests are subjected to seasonally dry periods leading to midday stomatal closure (Mulkey & Wright 1996), seasonal leaf loss in certain species (Wright 1996), or altered canopy structure due to wilting (Chiariello *et al.* 1987). Combined with the vast area of tropical forests, these physiological and morphological responses to seasonal drought could exert significant control over regional- and continental-scale climate, largely through the influence of stomatal behavior, albedo, and canopy-atmosphere coupling on the balance between latent and sensible heat. This possibility has been explored partly through theoretical analyses (*e.g.*, Shukla *et al.* 1990, Meinzer & Goldstein 1996, Sellers *et al.* 1996a), and direct studies of this scenario are warranted. Studies of upper-canopy physiology, however, have been hampered by difficulty of canopy access, particularly in the tropics. Recent advances in canopy access, which have included scaffolding towers (Sellers *et al.* 1995, 1997), and construction cranes (Parker *et al.* 1992), are now providing new opportunities for direct assessment of the physiological state of the upper canopy layers.

Many models of surface-atmosphere transport now include parameterizations for canopy physiology in their consideration of surface-atmosphere fluxes. Some of these models derive annual net photosynthetic CO₂ flux (NPP) from a consideration of radiation absorption (APAR) and environmental or physiological processes that restrict the efficiency of conversion of radiation to fixed carbon (*e.g.*, Potter *et al.* 1994, Prince & Goward 1995, Sellers *et al.* 1996a). This approach is based on the relationship derived by Monteith

(1977), who defined NPP as a function of efficiency and absorbed radiation, integrated over the growing season

$$\text{NPP} = \varepsilon * \int \text{APAR} \cdot dt, \quad (1)$$

where APAR indicates the amount of photosynthetically active radiation (PAR) absorbed by the vegetation canopy and epsilon (ε , sometimes called “dry matter yield”) represents the efficiency of converting this absorbed radiation to fixed biomass. This simple equation provides a useful framework for analyzing vegetation function because it partitions NPP into a physiological component (ε) and physical component (APAR). The utility of this equation also derives from the fact that absorbed radiation (the APAR term) can be assessed by commonly used remote vegetation indices, including the “simple ratio” (SR) and the “normalized difference vegetation index” (NDVI). These indices, which are derived from reflectance in the red and near-infrared regions of the spectrum, provide an estimate of green canopy display, and thus of *potential* photosynthetic activity (Kumar & Monteith 1981, Asrar *et al.* 1984, Hatfield *et al.* 1984, Sellers 1985, Bartlett *et al.* 1990, Gamon *et al.* 1995).

Assessment of ε has proven more difficult, and at the scale of a single stand is often accomplished indirectly by determining absorbed radiation (APAR) and harvesting the biomass accumulated over a growing season (*e.g.*, Joel *et al.* 1997), an approach that is usually impractical for forest vegetation. Consequently, some models have assumed a constant efficiency (*e.g.*, Heimann & Keeling 1989, Myneni *et al.* 1995) or derive this term from literature values by biome type (*e.g.*, Ruimy *et al.* 1994), rather than from direct measurement. However, an abundance of recent studies indicate that efficiency can vary substantially in time and space (Running & Nemani 1988, Runyon *et al.* 1994, Gamon *et al.* 1995, Joel *et al.* 1997). This departure from a fixed efficiency is often associated with periodic environmental and physiological limitations, which reduce stomatal aperture and carbon accumulation rates over the short term, thereby restricting NPP in the longer term. This view of a varying efficiency is in agreement with an abundance of ecophysiological literature documenting “downregulation” of photosynthesis, *i.e.*, periods of stomatal closure and reduced carbon uptake, when vegetation is exposed to adverse environmental conditions. A good example is the “midday photosynthetic depression” that has been well documented in the ecophysiological literature, particularly for plants exposed to warm, dry conditions (Tenhunen *et al.* 1987). Studies of stomatal behavior indicate that tropical forests may be particularly susceptible to midday stomatal closure during seasonal drought (Mulkey & Wright 1996). Direct, real-time assessment of efficiency in these forests may help us understand the potential impact of individual canopy responses on overall surface-atmosphere fluxes.

Recent studies have found that, over short time periods, photosynthetic light-use efficiency can be assessed using optical remote sensing. In particular, the photochemical reflectance index (PRI) functions over the short term as an index of xanthophyll cycle pigment activity (Gamon *et al.* 1992, 1997; Gamon & Surfus 1999), and varies with instantaneous photosynthetic light-use efficiency at

the leaf (Gamon *et al.* 1992, 1997; Peñuelas *et al.* 1995), canopy (Gamon *et al.* 1992, Styliniski *et al.* 2002), and stand (Nichol *et al.* 2000, Peñuelas & Inoue 2000, Rahman *et al.* 2001) scales. Based on these observations, recent studies have developed instantaneous versions of the light-use efficiency model for canopies and stands with promising results (Gamon *et al.* 2001; Rahman *et al.* 2001, 2004). These models are based on a revised formulation of Eq. 1 that defines the instantaneous leaf and canopy photosynthetic rate as a function of radiation-use efficiency and absorbed light as follows:

$$\text{photosynthetic rate} = \epsilon' * \text{APAR} \quad (2)$$

where photosynthetic rate is the instantaneous photosynthetic flux (carbon uptake, in $\mu\text{moles carbon m}^{-2} \text{ s}^{-1}$), APAR is the PAR absorbed by the canopy (incident PAR \times fraction of incident PAR absorbed), and ϵ' is the instantaneous photosynthetic radiation-use efficiency (the efficiency of converting absorbed radiation into fixed carbon). Although this simple model closely approximates the net photosynthetic rate under certain conditions (Gamon *et al.* 2001), it may be more appropriate to consider this a measure of gross photosynthesis, particularly when applied to whole stands, because it does not explicitly consider ecosystem respiration. Because the efficiency term can be detected with spectral reflectance, it is now possible to use remote sensing to detect temporal and spatial variations in photosynthetic light-use efficiency. This approach has been widely tested at leaf and canopy scales (*e.g.*, Gamon *et al.* 1992, 1997, 2001) but has only recently been explored on whole forest stands (*e.g.*, Nichol *et al.* 2000, Rahman *et al.* 2001), and has rarely been tested in tropical forests. Recently, using satellite data, Asner *et al.* (2004) found that narrow-band reflectance indices of physiological function, including the PRI, responded to experimental drought treatment applied to an Amazon forest stand. These findings suggested that this index might provide a useful remote measure of photosynthetic light-use efficiency in tropical forest canopies. However, to our knowledge, the link between PRI and light-use efficiency has not been explicitly tested in tropical forests at leaf and canopy scales (the scales at which reflectance indices can be most directly linked to physiological measurements).

A primary goal of this study was to evaluate the diversity among species in behavior of APAR and ϵ' during drought. Our primary objective was to assess directly the validity of remote vegetation indices as measures of canopy light absorption (APAR), which, to our knowledge, has not been fully explored for tropical forests. A second objective was to explore optical detection of photosynthetic downregulation and associated declines in instantaneous photosynthetic light-use efficiency (ϵ'). Our main focus was on the canopy "skin," the uppermost canopy region visible from above and therefore most accessible to remote optical detection. A further, technical objective was to develop an optical sampling approach that could be applied under prevailing light conditions, which often preclude optical remote sensing due to the frequent cloud cover in this region of the world. By investigating the applicability of a light-use efficiency model without confounding atmospheric effects, the larger goal was to lay a foundation for improved estimation of carbon uptake by tropical forests from remote sensing.

METHODS

All measurements were made at the Smithsonian Institution's canopy crane site in Parque Metropolitan, Panama City, Panama, in April 1994, except for gas exchange, which was sampled in February and March, 1994 (see below). Annual precipitation averages approximately 1800 mm ($1781 \text{ mm} \pm 156 \text{ mm}$, mean \pm SD for 1995–2000), more than 90 percent of which occurs during the rainy season from May through December. Rainfall records at the site began in February 1994. In that year, it rained 5.2, 56.9, and 55.5 mm in February, March, and April, respectively. Thus, this study was conducted towards the end of the dry season at a time when soil water deficits were most extreme.

The forest was a 100–150 yr old second growth stand with tree heights up to 40 m. We used a 42 m tall tower crane with a 51 m jib to reach the upper canopy (Parker *et al.* 1992). Consequently, measurement periods were often limited by the availability of crane time. Study species are listed in Table 1.

PHOTOSYNTHETICALLY ACTIVE RADIATION (PAR) READINGS.—PAR, measured as incident photosynthetic photon flux density (PPFD), was sampled with a quantum sensor (LI-190, Li-Cor Inc, Lincoln, Nebraska, USA). In some cases, PPFD was also estimated from downwelling irradiance measurements integrated over the PAR (400–700 nm) region (see spectral reflectance, below).

GAS EXCHANGE.—For two dominant canopy tree species (*Luehea seemannii* and *Anacardium excelsum*), diurnal change in photosynthetic CO_2 exchange rates was measured for top canopy leaves in February (5 d) and March 1994 (2 d). Sampled leaves were marked at the time of their emergence. Leaves of physiologically optimal age (30–120 d old) were selected on unshaded branches. In a given day of sampling, we randomly selected five to eight leaves from this marked pool, and measured *in situ* net photosynthetic rates and conductance repeatedly with a portable infrared gas analyzer for CO_2 and water vapor (CIRAS, PP Systems, UK) under ambient light and humidity. Measurements were started *ca* 0700 h each day, and the same leaf was measured repeatedly at an interval of 0.5–2 h until 1800 h. Instantaneous gas exchange rates were recorded as soon as they were stable, usually between 3 and 6 min after enclosing the leaf in the cuvette. Leaves were kept at their natural orientation during the measurement, and PPFD at the leaf surface was recorded. Vapor pressure of ambient air (VP) and leaf temperature (T_L) varied throughout the day (1.7–2.7 KPa, and 28–36°C, respectively). The reference CO_2 concentration was regulated with a CO_2 mixer at 350 ppm (mean \pm SD = 349 ± 8.5 ppm).

Instantaneous *in situ* gas exchange rates reflect intrinsic physiological traits of the leaf, as well as multiple environmental factors that interactively vary with time. One way to explore a large *in situ* dataset that includes correlated factors is via multiple regressions. While regressions cannot necessarily establish causality, these can be used to evaluate the relative importance of extrinsic and intrinsic factors in predicting gas exchange parameters via standardized partial correlation coefficients (Shiple 2000). Our goal was to explore the factors that decouple *in situ* photosynthetic rates from the

TABLE 1. Descriptions of the nine study species. With the exception of the two obligately drought-deciduous species (*Pseudobombax* sp. and *Maclura* sp.), all canopies were in leaf during the time of this study. Nomenclature follows Croat (1978).

Plant species	Description
<i>Anacardium excelsum</i> (Berterp & Balb.) Skeels	brevideciduous (for perhaps 3 d in late December)
<i>Carica papaya</i> L.	facultatively dry-season deciduous (drops leaves as drought develops)
<i>Cecropia longipes</i> Pitt.	facultatively dry-season deciduous (drops leaves as drought develops)
<i>Enterolobium cyclocarpum</i> (Jacq.) Griseb.	brevideciduous (for perhaps 3 weeks in late February to early March)
<i>Ficus insipida</i> Willd.	evergreen tree
<i>Luehea seemannii</i> Tr. & Planch.	facultatively dry-season deciduous (drops leaves as drought develops)
<i>Piper reticulatum</i> L.	evergreen shrub or tree
<i>Pseudobombax septenatum</i> (Jacq.) Dug.	obligately dry-season deciduous (leaves drop in the first weeks of the dry season)
<i>Maclura tinctoria</i> (L.) D. Don ex Steud	obligately dry-season deciduous (leaves drop in the first weeks of the dry season)

rate predicted by PAR alone, and to relate this information to the light-use efficiency concept (Eq. 2). We used a statistical model that employed a series of multiple regressions based on the known theoretical and empirical relationship among relevant environmental variables and gas exchange parameters. The results of this model are illustrated in a path diagram (Fig. 6 in Results, below) that summarizes the relative importance of selected variables and their interactions in predicting the dependent variable of our interest, the net carbon assimilation rates. In this diagram, each relationship is indicated by a path coefficient, which is a standardized partial regression coefficient indicating how much change in the dependent variable (relative to its standard deviation) is associated with a unit change in the independent variable (relative to its standard deviation). Thus, a path coefficient represents the relative strength of a given factor in predicting another factor. Our approach follows the original path analysis developed by Sewell Wright (Mitchell 1993), but does not test the model's causal structure because our data are not suitable for such tests due to latent (unmeasured) variables and nonlinear relationships among some of the variables (Shipley 2000).

Specifically in our model, net photosynthetic rates (A) were examined as a function of PPF, g_s and the maximum photosynthetic rates observed for each leaf (A_{max}) that represents the inherent photosynthetic capacity of the leaf. Stomatal conductance (g_s) was examined as a function of PPF, VP and T_L . The combined effect of VP and T_L reflect the vapor pressure gradient between the leaf mesophyll and the ambient air. The effects of time of day on PPF and VP, as well as the joint effect of time of day and PPF on T_L were also examined. Although evapotranspirational cooling should affect the leaf temperature, the reciprocal effect of g_s on leaf temperature was ignored in this path model. This was because a separate multiple regression model examining the joint effect of PPF, Time, VP and g_s on T_L indicated that g_s and VP had smaller contributions than PPF or Time (not shown). Only the results for February measurements are reported below because the results of March gas exchange measurements were very similar in terms of both environmental factors and their relationship with gas exchange rates.

CHLOROPHYLL FLUORESCENCE.—To provide an indicator of photosynthetic radiation-use efficiency, leaf fluorescence measurements were made on three species under ambient conditions with a pulse-amplitude modulated fluorometer equipped with a leaf clamp (PAM-2000, Heinz Walz GmbH, Germany). These three species included two large, top-canopy trees (*A. excelsum* and *L. seemannii*) and one small (<6 m tall) tree (*P. reticulatum*). *Piper reticulatum* is normally an understory species, but in this case was located in a gap and was thus fully sun exposed. Fluorescence was expressed as $\Delta F/F_m'$, a measure of PSII radiation-use efficiency (Genty *et al.* 1989).

SPECTRAL REFLECTANCE.—Canopy spectral reflectance was determined with a pair of spectral detectors (model SE590 with detector model CE390WB-R, Spectron Engineering, Denver, CO) mounted on a self-leveling plate. These detectors sampled between 368.4 and 1113.7 nm at a 2.6 to 3.2 nm sampling interval, and a 10 nm bandwidth (full width half maximum). One detector sampled upwelling canopy radiance with a 15 degree FOV foreoptic, and the other sampled downwelling irradiance with a hemispherical diffuser foreoptic (Spectron Engineering, Denver, CO). The detector mounting plate was attached to a boom extended out the side of the gondola (Fig. 1). The gondola was then positioned above each individual canopy (for measuring top-canopy reflectance of individual species) or lowered through the canopy (to obtain within-canopy reflectance profiles). For top-canopy reflectance, the instruments were approximately 4 m above the canopy, yielding a sampling area of approximately 1 m in diameter at the top-canopy surface. To normalize for changing sky conditions under variable clouds, upwelling canopy radiance was normalized by the time-averaged downwelling irradiance, measured both immediately before and after each radiance scan. Downwelling irradiance was later cross-calibrated to upwelling radiance from a 99 percent reflective standard panel (Spectralon, Labsphere Inc., North Dutton, NH, USA) to provide correction to reflectance:

$$\text{reflectance} = (\text{canopy radiance/sky irradiance}) \times (\text{sky irradiance/panel radiance}). \quad (3)$$

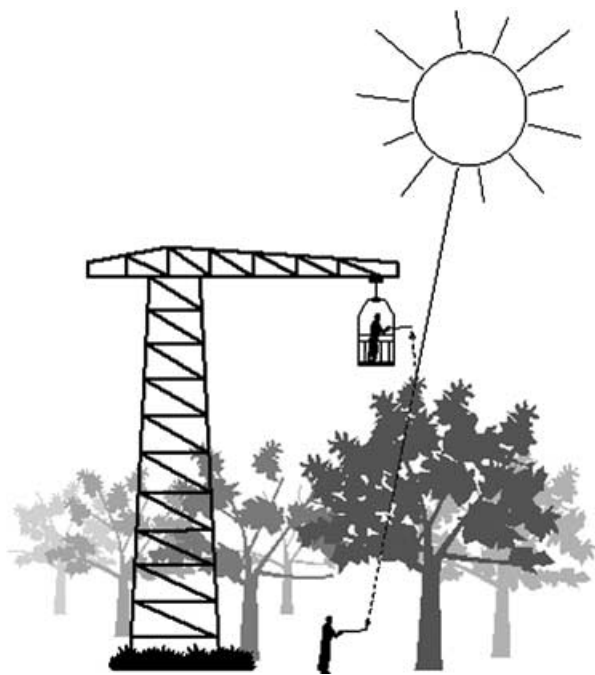


FIGURE 1. Schematic diagram illustrating method for obtaining canopy absorptance and reflectance. A pair of spectroradiometers mounted on the end of a boom above the canopy were used to calculate canopy spectral reflectance. Simultaneous below-canopy measurements with a line PPF sensor, combined with the above-canopy radiation measurements, were used to calculate whole-canopy absorptance. See text in Methods for further details.

Leaf spectral reflectance was measured with a leaf “reflectometer,” which consisted of the same portable spectrometer used for canopy reflectance, but modified for leaf reflectance measurements in the field. This configuration, which was previously described by Gamon *et al.* (1993), consisted of a light source, a bifurcated fiber optic probe (#2555.04, Fostec Inc., Auburn NY) attached to a leaf clamp, and the same spectral detector used for canopy reflectance (model SE590 with detector model CE390WB-R, Spectron Engineering). Leaf reflectance spectra were calculated by dividing the spectral radiance of the adaxial leaf surface by the radiance of a 99 percent reflective white standard. Following previous protocols (Peñuelas *et al.* 1995, Gamon *et al.* 1997), the PRI was determined from leaf reflectance of top-canopy leaves as follows:

$$\text{PRI} = (R_{531} - R_{570}) / (R_{531} + R_{570}) \quad (4)$$

where R_{531} indicates reflectance at 531 nm (the waveband of the “xanthophyll signal”), and R_{570} indicates reflectance at 570 nm (a reference waveband) (Gamon *et al.* 1993, 1997).

To calculate the broadband vegetation indices SR and NDVI, we simulated bands 1 (red: approximately 560 to 685 nm) and 2 (near-infrared: approximately 705 to 990 nm) of the Advanced Very High Resolution Radiometer (AVHRR), an imaging spectrometer on a US National Oceanographic and Atmospheric Administration (NOAA) satellite, using a full convolution as previously described in

Gamon *et al.* (1995). These bands have been widely used for the calculation of global vegetation indices for the purposes of monitoring APAR and potential photosynthetic activity of terrestrial vegetation (*e.g.*, Tucker *et al.* 1986, Myneni *et al.* 1995). After calculation of reflectance, SR and NDVI were then determined from these bands as follows:

$$\text{SR} = R_2 / R_1, \quad (5)$$

$$\text{NDVI} = (R_2 - R_1) / (R_2 + R_1), \quad (6)$$

where R_2 is the simulated reflectance in AVHRR band 2 and R_1 is the simulated reflectance in AVHRR band 1.

CANOPY STRUCTURE AND LIGHT ABSORPTION.—Leaf orientation was determined with a clinometer (Dasco Pro, Rockford, IL, USA). The position of horizontal leaves was defined as zero degrees, and vertical leaves as 90 degrees. Leaf angles reported here are absolute values, and thus do not distinguish between upward- or downward-tilting leaves.

Fractional absorptance or interception of PAR (F_{APAR} or F_{IPAR}) by vegetation was measured by sampling the upwelling and downwelling PAR fields both below and above the canopy as illustrated in Fig. 1. Reflectance measurements of bare soil were defined as having a reference F_{APAR} value of zero. Upwelling and downwelling below-canopy measurements were made with a light bar (SF-80, Decagon, Pullman WA) calibrated against a quantum sensor (LI-190SB, LI-COR, Lincoln NE), which provided broadband measurements of PAR. Simultaneous upwelling and downwelling above-canopy measurements were made with a pair of spectral detectors mounted on a self-leveling boom from the gondola (see “spectral reflectance” above). Photosynthetic photon flux density (PPFD) values were calculated by calibrating spectral irradiance (or radiance) between 400 and 700 nm using a calibration lamp (1800-02, LI-COR, Lincoln NE). This calibration to PAR irradiance was then confirmed in the field with the same quantum sensor (LI-190SB, LI-COR, Lincoln NE) used for light bar calibrations.

Fractional interception (F_{IPAR}) and fractional absorptance (F_{APAR}) were calculated from downwelling PAR radiation (I_{D}) and upwelling PAR radiation (I_{U}) both above (A) and below (B) the canopy as follows:

$$F_{\text{IPAR}} = (I_{\text{D,A}} - I_{\text{D,B}}) / I_{\text{D,A}}, \quad (7)$$

$$F_{\text{APAR}} = [(I_{\text{D,A}} + I_{\text{U,B}}) - (I_{\text{U,A}} + I_{\text{D,B}})] / (I_{\text{D,A}} + I_{\text{U,B}}). \quad (8)$$

RESULTS

Canopy spectral reflectance varied considerably across species, primarily due to the wide variation in green leaf cover in this forest during the dry season (Table 1). The canopy spectrum for *Anacardium excelsum*, one of the tallest species in full leaf at the site, yielded very low visible reflectance (400–700 nm), a high near-infrared reflectance (>700 nm), and a striking “red-edge” feature

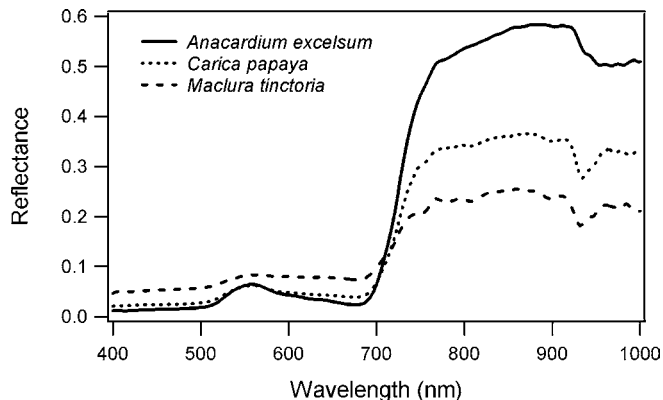


FIGURE 2. Canopy spectral reflectance for three representative species with contrasting habits and canopy structures: *Anacardium excelsum* (a dominant evergreen), *Carica papaya* (a small gap species with a sparse canopy), and *Maclura tinctoria* (a dominant drought-deciduous species).

near 700 nm (solid line, Fig. 2). By contrast, canopies of *Maclura tinctoria*, a large deciduous species that was leafless at the time, yielded a relatively high visible reflectance and a low near-infrared reflectance, and a shallow slope at the red edge (long dashes, Fig. 2). *Carica papaya*, a small gap species with a relatively sparse canopy, yielded a canopy reflectance spectrum that was intermediate between that of the fully green *Anacardium* sp. and the deciduous *Maclura* sp. (small dashes, Fig. 2).

Across species, the SR and NDVI yielded strong correlations with the fraction of absorbed PAR (F_{APAR} , Fig. 3). As has been previously reported for other ecosystems (Gamon *et al.* 1995), the relationship between NDVI and F_{APAR} saturated for dense green canopies, whereas the SR and F_{APAR} relationship was linear over the entire range of canopy densities encountered at this site. The two drought deciduous species, *Pseudobombax septenatum* and *Maclura* sp., clearly fell off the regression lines for the evergreen species. This departure indicated a relatively high amount of light absorption despite a relatively low percentage of green leaves visible from above in these canopies, both of which were leafless at the time of measurement. It was unclear from these whole-stand measurements how much of the light absorption was due to absorption by the leafless canopy overstory, and how much was due to absorption by the dense cover of evergreen understory species, which were largely invisible from our instruments positioned above the forest.

Physiological performance among species at this site also varied widely. For example, two of the evergreen trees, *Anacardium excelsum* and *Luehea seemanii*, yielded dramatically different diurnal photosynthetic responses (Fig. 4). Although both species were exposed to similar midday illumination (Fig. 4a), leaves of *Luehea* sp. had much higher levels of maximum CO_2 uptake and stomatal conductance (Figs. 4b, c). *Anacardium* sp. exhibited maximal photosynthetic rates in midmorning, followed by a depression during peak irradiance. By contrast, *Luehea* sp. exhibited diurnal photosynthetic rates more closely matching the incident PPFD pattern.

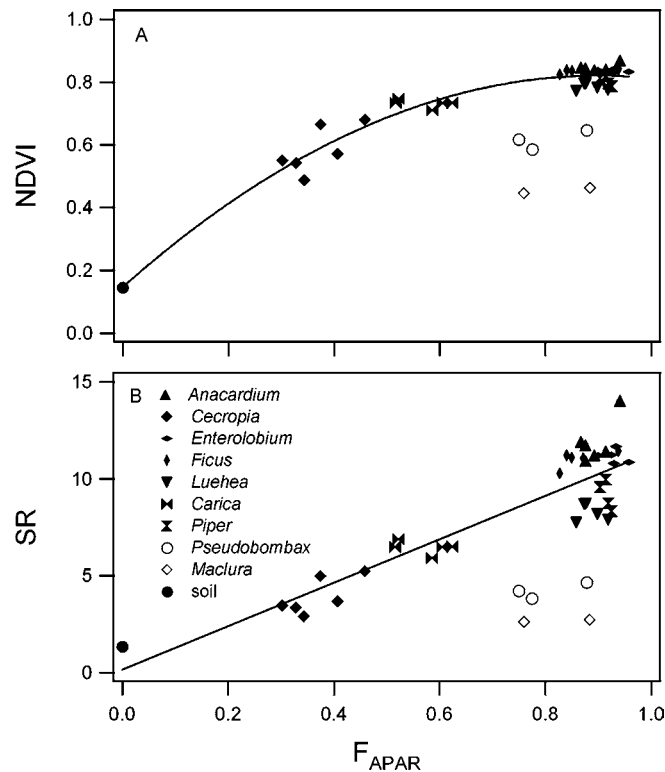


FIGURE 3. Relationship between NDVI (panel A) or SR (panel B) and the fraction of absorbed photosynthetically active radiation (F_{APAR}) for individual canopies or bare soil (see legend). Lines represent best fits for all points excluding the drought-deciduous canopies (indicated by open symbols).

In both species, stomatal conductance exhibited an asymmetrical pattern, with maximal rates in the morning followed by a steady decline through the afternoon (Fig. 4c).

The generality of these leaf responses was examined for the pooled data for 5 d in February ($N = 15$ leaves for *Anacardium* sp. and $N = 17$ leaves for *Luehea* sp.). These contrasting photosynthetic responses can be visualized by examining the assimilation rate as a function of PPFD and stomatal conductance. *Luehea* sp. leaves saturated with light at higher PPFD and had a higher maximum assimilation rate than *Anacardium* sp. leaves (Figs. 5a, b). The large scatter in assimilation rate for a given level of PPFD reflects varying degrees of stomatal limitation and PS II downregulation, as well as differences among leaves in their photosynthetic capacity (see discussion of Fig. 6, below). The generally lower stomatal conductance in *Anacardium* sp. (Figs. 5c, d) suggests a greater stomatal limitation and midday depression of photosynthesis in *Anacardium* sp. than in *Luehea* sp.

The path diagram (Fig. 6) summarizes the effects on stomatal conductance of environmental factors that varied with time of day, as well as the interactive effect of PPFD and conductance on photosynthetic rates. PPFD at the leaf surface was a function of the time of day in a convex form, although there was a large variance at a given time due to cloud cover and leaf orientation, resulting in

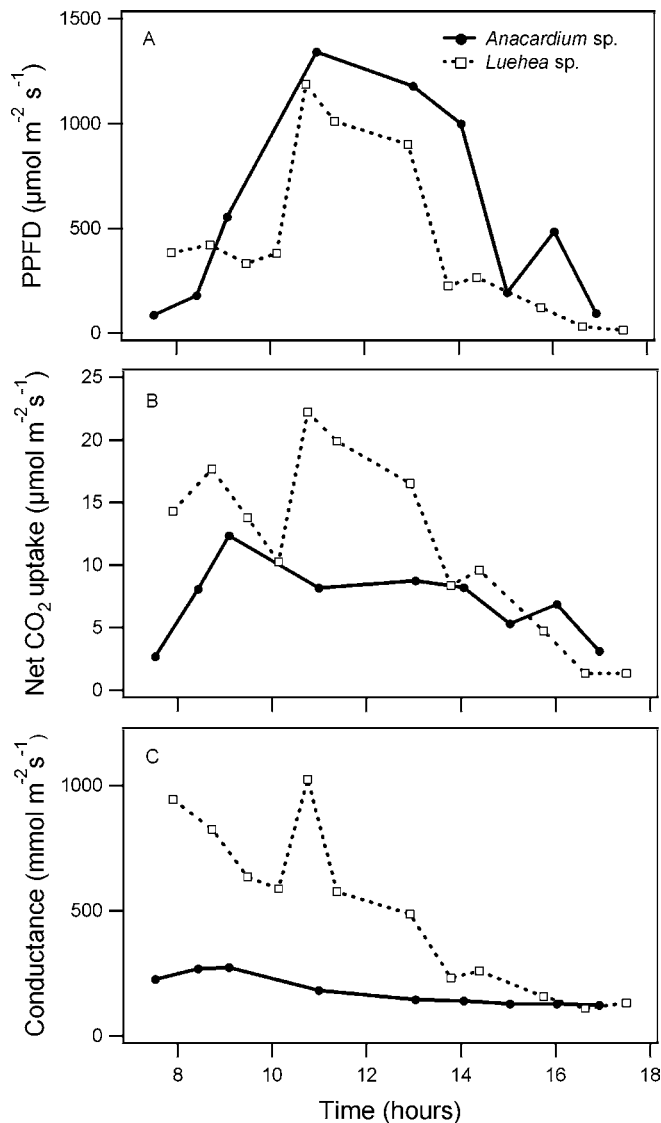


FIGURE 4. Diurnal patterns of incident PPFD, net CO₂ uptake, and stomatal conductance for representative leaves of *Anacardium excelsum* and *Luehea seemannii*, measured in February 1994.

its weak relationship with time. In contrast, vapor pressure of the atmosphere declined linearly with time of the day. Leaf temperature, which affects the vapor pressure deficit between the leaf and atmosphere, was better predicted by the combination of PPFD and Time ($R^2 = 0.48$ and 0.67 for *Anacardium* sp and *Luehea* sp., respectively) than by either variable alone. Leaf temperature had a strong negative effect on stomatal conductance in both species, while PPFD and vapor pressure of the atmosphere had positive effects on stomatal conductance. The relationships among most variables included in the model were similar for the two species. However, photosynthetic rates and stomatal conductance of *Luehea* sp. tracked the PPFD more closely than *Anacardium* sp., as indicated by its much stronger path coefficient of PPFD on A and g_s . In *Anacardium*

sp. (but not *Luehea* sp.) photosynthetic rates were strongly limited by its inherently low A_{\max} , which must require energy dissipation *via* other mechanisms besides carboxylation (*e.g.*, heat dissipation) under high PPFD. This dissipation was linked to a greater degree of midday photosynthetic downregulation, detectable as a greater reduction in PSII light-use efficiency measured by $\Delta F/F_m'$ (Figs. 7 and 8).

The widely varying morphological and physiological responses to dry season conditions of species at this site are further illustrated in Figure 7, which illustrates diurnal incident PPFD, leaf angle, and $\Delta F/F_m'$ values for three evergreen species: *Piper reticulatum*, *Anacardium excelsum*, and *Luehea seemannii*. Although all three had similar diurnal irradiance patterns (Fig. 7a), *Piper* sp. exhibited a dramatic midday leaf wilting, *Luehea* sp. exhibited a subtle alteration in leaf angle, and *Anacardium* sp. had no detectable change in leaf orientation (Fig. 7b). *Piper* sp. and *Anacardium* sp., the two species with "opposite" leaf orientation responses to midday drought (Fig. 7b), had remarkably similar $\Delta F/F_m'$ patterns, indicating a considerable reduction in midday PSII light-use efficiency (Fig. 7c). By contrast, *Luehea* sp., which had the intermediate leaf angle response, exhibited almost no midday decline in $\Delta F/F_m'$ (Fig. 7c). $\Delta F/F_m'$ was clearly much less sensitive to increasing light in *Luehea* sp. than in the other two species (Fig. 8), further confirming the relative lack of midday downregulation in this species.

The contrasting diurnal patterns of leaf orientation in these three species (Fig. 7b) were associated with contrasting diurnal canopy reflectance patterns. *Piper* sp., the species with a dramatic midday leaf wilting, also had a significant midday decline in NDVI (not shown) and SR (Fig. 9) because wilting reduced the green leaf area visible to the sensor at midday. By contrast, *Luehea* sp. and *Anacardium* sp., both of which exhibited less diurnal leaf movement, showed far less diurnal change in NDVI or SR (Fig. 9).

To examine the ability of narrow-band reflectance to detect midday downregulation of PSII light-use efficiency, we sampled leaf reflectance with the leaf reflectometer in *Anacardium* sp., one of the evergreen species exhibiting dramatic midday declines in $\Delta F/F_m'$. The PRI of *Anacardium* leaves was strongly correlated with $\Delta F/F_m'$, and both measures of PSII light-use efficiency declined substantially toward midday (Fig. 10). By contrast, *Luehea* sp., which exhibited little midday downregulation (Figs. 4–8), had no significant correlation between PRI and $\Delta F/F_m'$ (not shown).

To examine the spatial distribution of midday PSII downregulation, we sampled incident PPFD and canopy reflectance near midday at four levels in an *Anacardium* sp. canopy: 1) top canopy; 2) mid crown; 3) below crown; and 4) just above the understory by lowering the gondola through the canopy. As expected, the top-canopy region with the highest PPFD levels ($1629 \mu\text{mol}/\text{m}^2/\text{s}^{-1}$) had the lowest PRI values (Fig. 11), indicating PSII down-regulation in this sun-exposed canopy region. By contrast, the deep canopy layers and the understory maintained PRI values similar to the morning values of the sun-exposed canopy (*cf.* Fig. 10), indicating little reduction in light-use efficiency in these shaded regions.

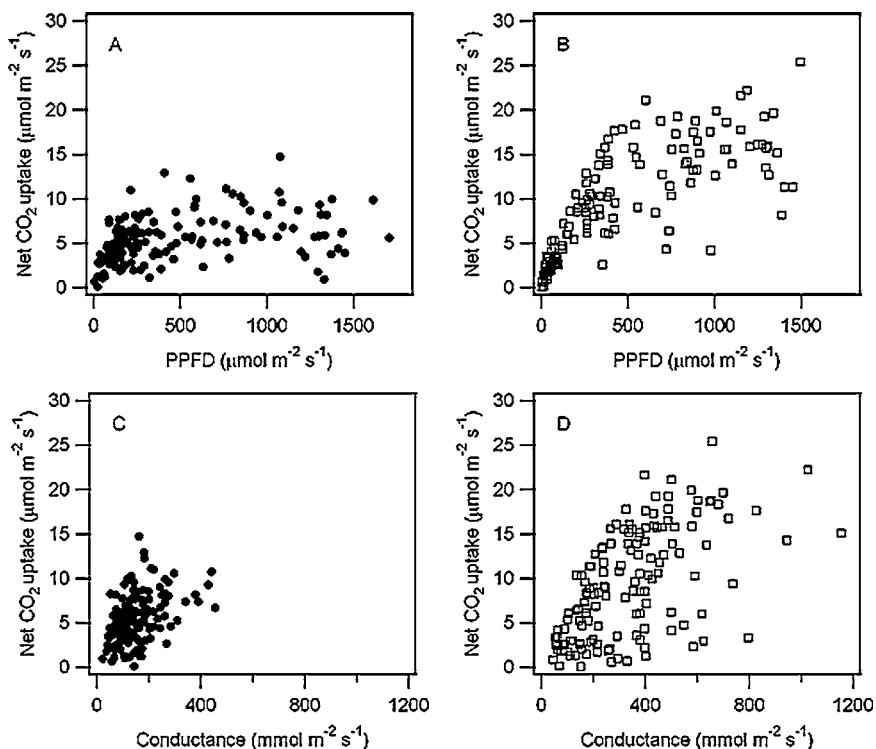


FIGURE 5. Relationships between *in situ* net CO₂ assimilation and incident PPFD (panels A and B) or stomatal conductance (panels C and D) for upper canopy leaves of *Anacardium excelsum* (panels A and C, $N = 15$ leaves) and *Luehea seemannii* (panels B and D, $N = 17$ leaves) sampled over 5 d in February 1994.

DISCUSSION

The measurements presented here indicate remarkable morphological and physiological diversity among the species at this forest site. Diversity in canopy structure is evident in the wide-ranging patterns of spectral reflectance, SR, and NDVI, which indicate large differences in foliar density, and PAR absorption. Additional structural diversity is also apparent in the divergent diurnal leaf angle responses of three species during a dry, sunny day, which were also detectable remotely. Because all these structural and morphological responses influence canopy light absorption (F_{APAR}), an important determinant of canopy photosynthesis (Eq. 2), they could have a profound impact on overall stand fluxes. In the case of canopies in full leaf, the broadband indices SR and NDVI can accurately estimate fractional PAR absorption (F_{APAR}), supporting the use of these reflectance indices as measures of potential photosynthesis in tropical forests.

In Fig. 3, the significant departure of drought-deciduous species from the main regression could be explained in two possible ways. First, this departure could be an artifact of the measurement methods; because our methods integrated absorption over the full PAR region (400–700 nm), we could not distinguish between PAR absorbed by green canopy foliage and PAR absorbed by bare branches. It is possible that the relatively high F_{APAR} in these species was due to substantial branch absorptance, and that this light absorption was not detected by the vegetation indices, which largely scale with absorption by green canopy material. Secondly,

these drought deciduous canopies had a very dense understory of evergreen shrubs that contributed to the high F_{APAR} values, but were generally “invisible” to the spectroradiometer, which largely viewed the overtopping branches of the dominant deciduous trees. Although our measurements cannot distinguish these possibilities, it is likely that the vertical heterogeneity resulting from this complex, layered stand structure contributed to errors in estimating F_{APAR} from nadir reflectance measurements. This kind of nonuniform vertical structure is rarely treated in canopy radiative transfer models, most of which assume a homogenous spatial distribution of canopy elements (Goel 1988). Such errors in F_{APAR} estimates from remotely sensed vegetation indices could lead to substantial underestimates of forest fluxes for dry tropical forests having dense evergreen understory vegetation overlaid by deciduous tree canopies. In light of our inability to balance the terrestrial carbon budget and the substantial uncertainties associated with direct flux measurements in structurally complex tropical forest stands (Grace *et al.* 1995, Malhi & Grace 2000, Araújo *et al.* 2002, Carswell *et al.* 2002), the influence of layered forest canopies on light absorption and stand fluxes deserves further investigation. It should be possible to couple remote sensing with more detailed three-dimensional analyses of spectral reflectance and absorptance. Such a study might benefit from new methods of sampling *spectral* absorption instead of integrated broadband absorption, which may be useful in distinguishing the portion of PAR absorbed by green leaves from the portion absorbed by branches (Serrano *et al.* 2000).

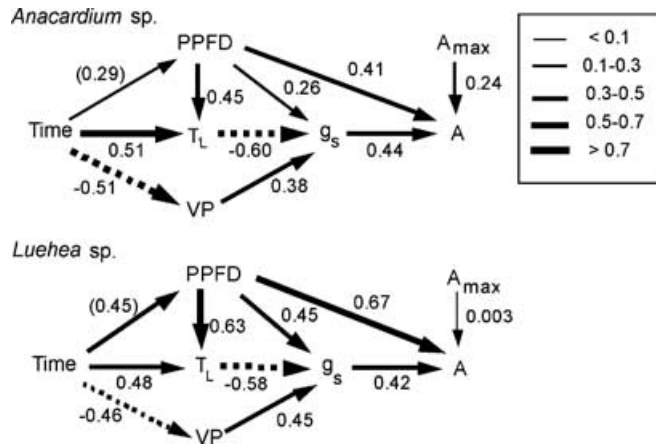


FIGURE 6. Path diagrams summarizing the interactive effects of time on environmental factors, and their effects on stomatal conductance (g_s) and net photosynthetic rates (A) for pooled gas exchange data of upper canopy leaves of *Anacardium* sp. ($N = 15$ leaves) and *Luehea* sp. ($N = 17$ leaves) collected throughout the day for total 5 d in February 1994. Each diagram was constructed by a series of multiple regressions. The predicted variable by each regression model is at the pointed tip of the arrows, while the predictive variables are at the arrow bases. The direction of an arrow often reflects the logical causal direction (e.g., PPFD affects the leaf temperature, but leaf temperature cannot affect PPFD), but not necessarily indicates a causal relationship or lack of feedback response. The width of an arrow corresponds to the number written by the arrow, which is the standardized partial regression coefficient, a statistical measure of the predictive power. The number in parentheses by the arrow connecting time and PPFD does not have a negative or positive sign unlike other path coefficients, because it is R for the second-order polynomial regression. See Appendix for the actual multiple regression equations.

In addition to structural diversity, species at this site displayed a considerable degree of diversity in photosynthetic responses, which was not necessarily linked to structural patterns. This physiological diversity was apparent in dramatically contrasting patterns of stomatal conductance, light-saturated CO_2 uptake, and PSII downregulation at midday. The SR and NDVI did not detect the photosynthetic downregulation apparent in one of the species of this site (*Anacardium* sp.). In contrast, downregulation in *Piper* sp. was correlated with leaf wilting, which was detectable as a decline in SR and NDVI. However, the midday SR values in *Piper* sp. were not significantly different from those of *Luehea* sp., which exhibited very high midday photosynthetic rates, high midday stomatal conductance, and very little evidence of PSII downregulation. Thus, in agreement with the recent findings of Asner *et al.* (2004) who examined drought impacts on an Amazonian forest stand, we conclude that satellite greenness indices alone (e.g., SR and NDVI) would not be able to detect differences in physiological behavior for complex tropical forest stands.

$\Delta F/F_m'$ proved to be a rapid and portable index of PSII downregulation at the leaf level, and was able to clearly distinguish different diurnal patterns of PSII activity in three species having very similar midday SR values. However, this fluorescence method is

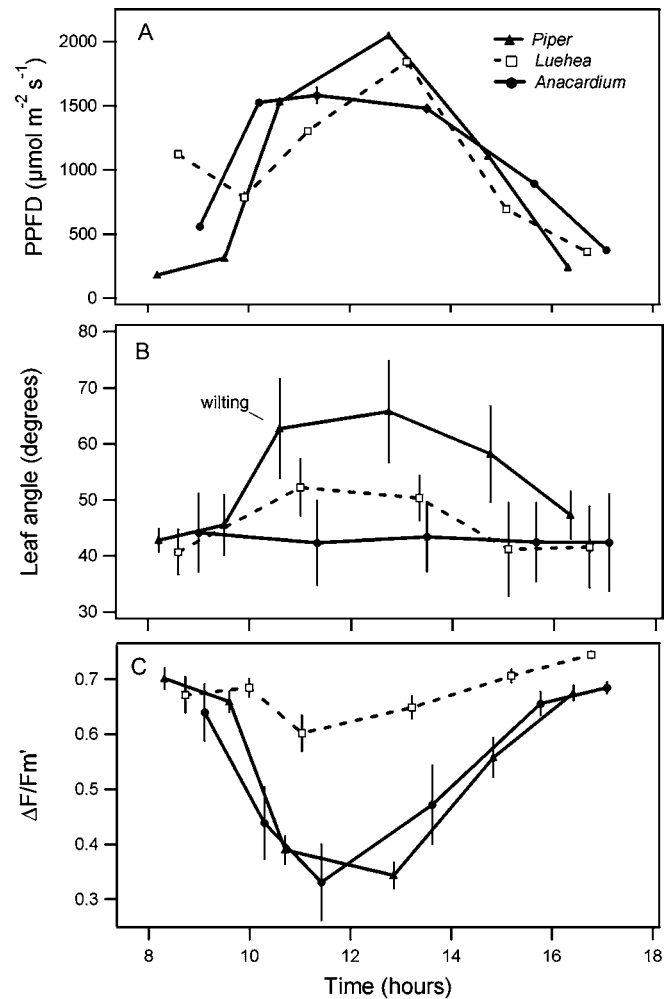


FIGURE 7. Diurnal course of downwelling PPFD at the canopy top (panel A), leaf angle (degrees from horizontal; panel B) and $\Delta F/F_m'$ (panel C), for *Anacardium excelsum*, *Luehea seemannii*, and *Piper reticulatum*. Each point in panels B and C represents the mean \pm SEM for six top-canopy leaves.

limited to close-range measurements of individual leaves due to the requirement for saturating light pulses needed to attain F_m' measurements. The reflectance index PRI, which reveals the activity of the xanthophyll cycle over diurnal time scales, showed promise as an index of PSII downregulation. In *Anacardium* sp. canopies, which lacked any detectable midday structural changes, this index exhibited a midday decline that was closely correlated with $\Delta F/F_m'$. A vertical profile indicated suppressed midday PRI values in the uppermost canopy layer exposed to full sun, most likely reflecting greater levels of photoprotective carotenoid (carotene and xanthophyll) pigments at the canopy top. These findings demonstrate that this index can reveal spatial and temporal patterns of photosynthetic downregulation during the dry season at both the leaf and canopy scales, and thus may provide a useful index of light-use efficiency in tropical forest stands. Similarly, Asner *et al.* (2004) reported that PRI

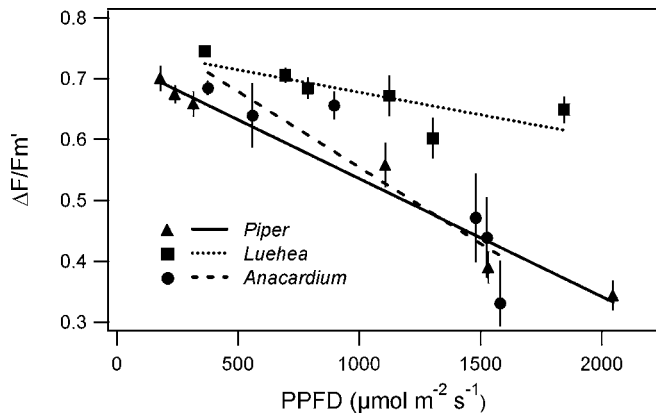


FIGURE 8. Light response of $\Delta F/F_m'$ for *Anacardium excelsum*, *Luehea seemannii*, and *Piper reticulatum* measured by sampling leaves at different times of day (derived from data in Fig. 7).

detected from satellite is sensitive to drought effects in an Amazonian forest.

The diversity of physiological and structural responses evident in this single forest stand reveals an aspect of tropical diversity that has generally not received the same attention as species diversity. Our findings are consistent with other recent studies from this and other similar sites that suggest a wide range of functional diversity exists within a single tropical forest stand (Mulkey *et al.* 1996, Wright 1996, Kitajima *et al.* 1997a). Furthermore, this diversity, and its associated optical properties, are likely to vary with successional stage (Kitajima *et al.* 2005). It is likely that the wide range in physiological and structural responses of the various tree species at this site have a significant impact on overall ecosystem biogeochemical processes, and that these responses are far more dynamic in time and space than is often assumed in flux models derived from remote sensing. These contrasting patterns of physiological and structural behavior within a single forest stand present challenges for remote estimation of carbon flux based primarily on absorbed radiation derived from satellite NDVI. A significant finding of this study is that

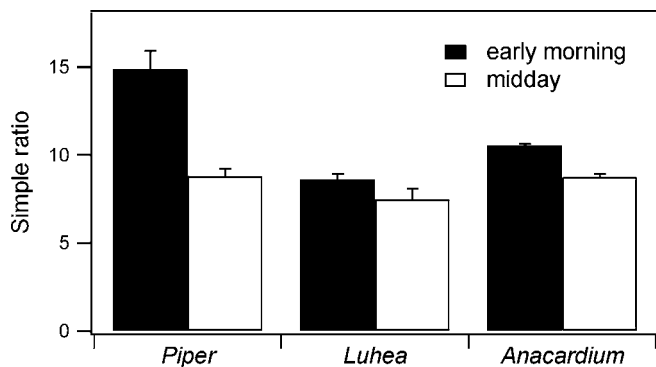


FIGURE 9. Simple ratio calculated for *A. excelsum*, *L. seemannii* and *P. reticulatum* canopies at early morning (0800–0900 h) and midday (1240–1330 h).

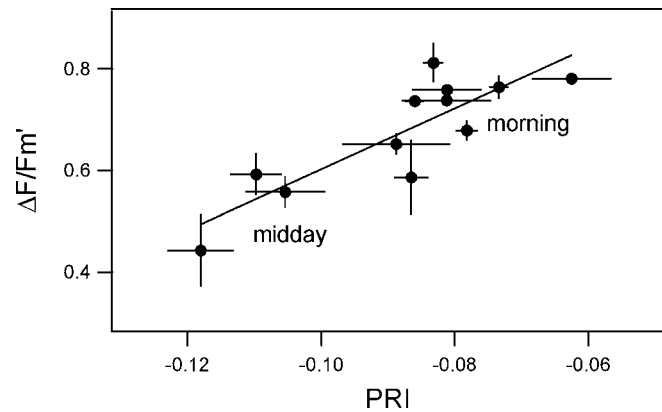


FIGURE 10. Relationship between PRI and $\Delta F/F_m'$ ($r=0.85$) for top canopy leaves of *Anacardium excelsum* sampled at several times of day between 0750 and 1330 h. Each point represents a mean \pm SEM of three samples per leaf.

this diversity can be addressed by a variety of novel optical measurements, suggesting that more refined remote sensing methods could be developed that directly assess this functional diversity.

Due to the wide variation in responses at this site, we recommend a variety of approaches to evaluate the impact of drought on ecosystem carbon fluxes of tropical forest stands. Clearly leaf gas exchange has been, and will continue to be, a valuable tool for

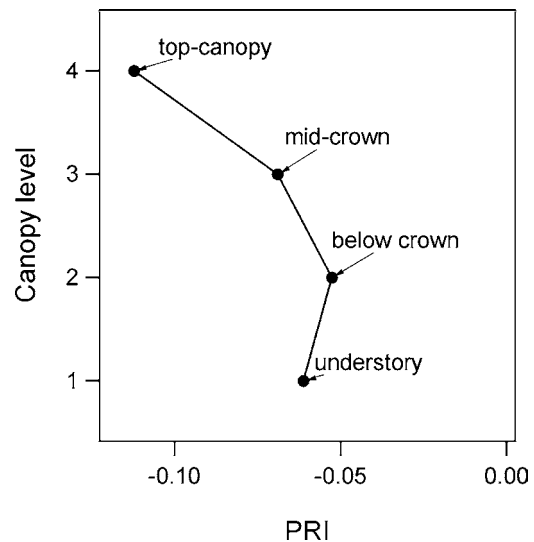


FIGURE 11. Vertical profile of PRI for an *Anacardium excelsum* canopy measured at four levels: (1) uppermost canopy region in full sun ("top canopy"), mid-canopy region in shade ("mid crown"), immediately below the lowest *Anacardium* sp. leaf layer but several meters above the understory ("below crown"), and 2 to 3 m above the understory layer ("understory"). Mean downwelling PPFD during reflectance measurements at the four levels were 1629, 351, 132, and 115 $\mu\text{mol}/\text{m}^2/\text{s}^{-1}$, respectively. Sampling was begun at 1350 h (top canopy) and completed at 1403 h (understory) and proceeded by gradually lowering the gondola through the canopy while sampling canopy reflectance.

exploring the range in physiological behavior of complex stands; however, an integrated whole-stand estimate is difficult to assemble from leaf gas exchange. One approach would be to utilize direct stand flux measurements via eddy covariance, as is now being done in many regions of the world (*e.g.*, Sellers *et al.* 1995, 1997; Malhi & Grace 2000; Valentini *et al.* 2000, Araújo *et al.* 2002). Unfortunately, eddy flux cannot resolve the contribution of different component fluxes to total ecosystem fluxes (Moncreiff *et al.* 1996), and thus may not be able to partition overall system fluxes into species, stand layers, or evergreen and deciduous components at mixed sites such as the one used in this study. Thus, a combination of measurements at a range of scales is still needed to more fully explore contributions of individual ecosystem components to the overall fluxes. At this time, the net impact of drought on tropical forest CO₂ flux remains unclear, in part due to site differences, interannual variability in rainfall, difficulty in resolving component fluxes, and the general problem of undersampling in the tropics, which is only now beginning to be addressed (*e.g.*, Araújo *et al.* 2002, Carswell *et al.* 2002).

The optical sampling methods presented here offer an additional set of tools for evaluating spatial and temporal variation that can help reveal important physiological and structural controls on system fluxes. Because optical methods can be used to parameterize the two terms in Eq. 2, they can provide a simple semi-empirical method for exploring spatial and temporal patterns of photosynthetic activity. Recently, using a light-use efficiency model derived from satellite imaging spectrometry, Asner *et al.* (2004) demonstrated that drought can have significant impacts on NPP in an Amazonian forest stand, but a direct link to physiological downregulation at leaf and canopy scales was not demonstrated in that study. To our knowledge, the utility of optical tools as indicators of midday downregulation of individual forest species has received little attention in tropical forest ecosystems, in part due to shortage of operational instruments and sampling platforms, and in part due to the difficulty of sampling under clouds. The use of dual detectors to correct for changing sky conditions is one way to overcome the limitation of clouds in tropical environments. Such dual-detector systems are now commercially available (*e.g.*, FieldSpec Pro Dual VNIR, Analytical Spectral Devices, Inc., Boulder CO, USA; SD2000, Ocean Optics, Dunedin, FL, USA; UniSpec DC, PP Systems, Amesbury MA, USA) and could greatly assist in providing accurate, hyperspectral reflectance measurements of individual tree canopies in cloudy regions of the world such as the tropics. Similarly, standardized leaf reflectance sampling is now possible with portable leaf reflectometers that enable rapid leaf measurement under any light conditions (*e.g.*, Gamon & Surfus 1999). Unlike gas exchange and eddy covariance methods, which cannot readily bridge leaf and stand scales, reflectance methods can be easily applied across scales (Gamon & Qiu 1999). In addition, "hyperspectral" (narrow-band) spectrometers that combine spectral detail with spatial detail sufficient to resolve within-stand variability would be very useful in scaling between leaf level and whole stand flux responses, particularly when used in combination with gas exchange methods. Such scaling studies could provide important validation for light-use efficiency models applying reflectance measurements from aircraft

or satellite (*e.g.*, Nichol *et al.* 2000; Rahman *et al.* 2001, 2004; Asner *et al.* 2004).

Recent campaigns to initiate ecosystem-scale flux sampling for tropical forest stands (*e.g.*, Grace *et al.* 1995, Malhi & Grace 2000, Araújo *et al.* 2002, Carswell *et al.* 2002) could provide new opportunities for validating the light-use efficiency model represented in Eqs 1 and 2. To do this, photosynthetic and respiratory flux methods would have to be supplemented with hyperspectral reflectance measurements at multiple spatial and temporal scales. Together, these approaches may offer new ways to explore the impact of periodic stresses on ecosystem carbon and water flux in tropical ecosystems. Novel instrumentation, including portable spectrometers (*e.g.*, Gamon & Surfus 1999) and aircraft-based spectrometers (*e.g.*, Nichol *et al.* 2000, Rahman *et al.* 2001) could be deployed in such a study. Such combined optical and flux measurements have been started in other regions of the world as part of SpecNet (Spectral Network, <http://vcsars.calstatela.edu/SpecNet/index.html>) but tropical sites remain underrepresented in this program at this time. Unfortunately, adequate instrumentation and canopy access remain a challenge for all but a handful of sites, particularly in the tropics. Clearly, improved instrumentation and canopy access provided by canopy cranes, towers, and light aircraft will continue to play an important role in revealing the controls on carbon fluxes of forested ecosystems.

ACKNOWLEDGMENTS

This paper is dedicated to the late Alan Smith whose vision and efforts enabled the canopy crane and inspired us to complete this project. Thanks also to Ron Johnson, Dave Horvath and the late John Caulfield for technical assistance in the construction of the reflectometer, to Dennis Kimura for Figure 1, and to Bill Shipley for advice on our multiple regression approach. This work was supported by grants from NSF (J. Gamon and S. Mulkey), NASA (J. Gamon), the Andrew W. Mellon Foundation (K. Kitajima and S. J. Wright), the Inter American Institute (IAI) for Global Change Research, and a Smithsonian fellowship (J. Gamon), which provided travel and logistical support for the fieldwork. L. Serrano acknowledges financial support from MCYT (Spain) during completion of this study.

LITERATURE CITED

- ARAÚJO, A. C., A. D. NOBRE, B. KRUIJT, J. A. ELBERS, R. DALLAROSA, P. STEFANI, C. VON RANDOW, A. O. MANZI, A. D. CULF, J. H. C. GASH, R. VALENTINI, AND P. KABAT. 2002. Comparative measurements of carbon dioxide fluxes from two nearby towers in a central Amazonian rainforest: The Manaus LBA site. *J. Geophys. Res.* DOI 10.1029/JD000676.
- ASNER, G. P., D. NEPSTAD, G. CARDINOT, AND D. RAY. 2004. Drought stress and carbon uptake in an Amazon forest measured with spaceborne imaging spectroscopy. *Proc. Natl. Acad. Sci.* 101: 6039–6044.
- ASRAR, G., M. FUCHS, E. T. KANEMASU, AND J. L. HATFIELD. 1984. Estimating absorbed photosynthetic radiation and leaf area index from spectral reflectance in wheat. *Agron. J.* 76: 300–306.

- BARTLETT, D. S., G. J. WHITING, AND J. M. HARTMAN. 1990. Use of vegetation indices to estimate intercepted solar radiation and net carbon dioxide exchange of a grass canopy. *Remote Sensing Environ.* 30: 115–128.
- CARSWELL, F. E., A. L. COSTA, M. PALHETA, Y. MALHI, P. MEIR, J. de P. R. COSTA, M. de L. RUIVO, L. do S. M. LEAL, J. M. N. COSTA, R. J. CLEMENT, AND J. GRACE. 2002. Seasonality in CO₂ and H₂O flux at an eastern Amazonian rain forest. *Journal of Geophysical Research*. DOI 10.1029/JD000623.
- CHIARIELLO, N. R., C. B. FIELD, AND H. A. MOONEY. 1987. Midday wilting in a tropical pioneer tree. *Funct. Ecol.* 1: 3–11.
- COLLINSON, A. S. 1988. *Introduction to World Vegetation*, 2nd Ed. Unwin Hyman, London, UK.
- CROAT, T. B. 1978. *The Flora of Barro Colorado Island*. Stanford University Press, Stanford, California.
- Gamon J. A., C. B. FIELD, A. L. FREDEEN, AND S. THAYER. 2001. Assessing photosynthetic downregulation in sunflower stands with an optically based model. *Photosynthesis Res.* 67: 113–125.
- , C. B. FIELD, M. L. GOULDEN, K. GRIFFIN, A. E. HARTLEY, G. JOEL, J. PEÑUELAS, AND R. VALENTINI. 1995. Relationship between NDVI, canopy structure, and photosynthesis in three Californian vegetation types. *Ecol. Appl.* 5: 28–41.
- , I. FILELLA, AND J. PEÑUELAS. 1993. The dynamic 531-nanometer Δ reflectance signal: A survey of twenty angiosperm species. *In* H. Y. Yamamoto and C. M. Smith (Eds.). *Photosynthetic responses to the environment*, pp. 172–177. American Society of Plant Physiologists, Rockville, Maryland.
- , J. PEÑUELAS, AND C. B. FIELD. 1992. A narrow-waveband spectral index that tracks diurnal changes in photosynthetic efficiency. *Remote Sensing of Environment.* 41: 35–44.
- , AND H.-L. QIU. 1999. Ecological applications of remote sensing at multiple scales. *In* F. I. Pugnaire, F. Valladares (Eds.). *Handbook of functional plant ecology*, pp. 805–846. Marcel Dekker, Inc., New York.
- , L. SERRANO, AND J. S. SURFUS. 1997. The photochemical reflectance index: An optical indicator of photosynthetic radiation-use efficiency across species, functional types, and nutrient levels. *Oecologia* 112: 492–501.
- , AND J. S. SURFUS. 1999. Assessing leaf pigment content and activity with a reflectometer. *New Phytol.* 143: 105–117.
- GENTRY, A. H. 1988. Changes in plant community diversity and floristic composition on environmental and geographical gradients. *An. Mo. Bot. Gard.* 75: 1–34.
- GENTY, B., J. -M. BRIANTAIS, AND N. R. BAKER. 1989. The relationship between the quantum yield of photosynthetic electron transport and quenching of chlorophyll fluorescence. *Biochimica et Biophysica Acta* 990: 87–92.
- GOEL, N. S. 1988. Models of vegetation canopy reflectance and their use in estimation of biophysical parameters from reflectance data. *Remote Sensing Rev.* 4: 1–212.
- GRACE, J., J. LLOYD, J. MCINTYRE, A. C. MIRANDA, P. MEIR, H. S. MIRANDA, C. NOBRE, J. MONCREIFF, J. MASSHEDER, Y. MALHI, I. WRIGHT, AND J. GASH. 1995. Carbon dioxide uptake by an undisturbed tropical rain forest in southwest Amazonia, 1992 to 1993. *Science* 270: 778–780.
- HATFIELD, J. L., G. ASRAR, AND E. T. KANEMASU. 1984. Intercepted photosynthetically active radiation estimated by spectral reflectance. *Remote Sensing Environ.* 14: 65–75.
- HEIMANN, M., AND C. D. KEELING. 1989. A three-dimensional model of atmospheric CO₂ transport based on observed winds: 2. Model description and simulated tracer experiments. *In* D. H. Peterson (Ed.). *Aspects of climate variability in the Pacific and the Western Americas*. AGU Monograph, 55, pp. 237–275. American Geophysical Union, Washington, DC.
- JOEL, G., J. A. GAMON, AND C. B. FIELD. 1997. Production efficiency in sunflower: The role of water and nitrogen stress. *Remote Sensing Environ.* 62: 176–188.
- KITAJIMA, K. S., S. S. MULKEY, AND S. J. WRIGHT. 1997a. Seasonal leaf phenotypes in the canopy of a tropical dry forest: Photosynthetic characteristics and associated traits. *Oecologia* 109: 490–498.
- , ———, AND ———. 1997b. Decline of photosynthetic capacity with leaf age in relation to leaf longevity for five tropical canopy tree species. *Am. J. Bot.* 84: 702–708.
- , ———, AND ———. 2005. Variation in crown light utilization characteristics among tropical canopy trees. *Ann. Bot.* 95: 535–547.
- KUMAR, M., AND J. L. MONTEITH. 1981. Remote sensing of crop growth. *In* H. Smith (Ed.). *Plants and the daylight spectrum*, pp. 133–144. Academic Press, London, England.
- MALHI, Y., AND J. GRACE. 2000. Tropical forests and atmospheric carbon dioxide. *Tree* 15: 332–337.
- MEINZER, F., AND G. GOLDSTEIN. 1996. Scaling up from leaves to whole plants and canopies for photosynthetic gas exchange. *In* S. S. Mulkey, R. L. Chazdon, and A. P. Smith (Eds.). *Tropical Forest Ecophysiology*, pp. 114–138. Chapman and Hall, New York.
- , J. L. ANDRADE, G. GOLDSTEIN, N. M. HOLBROOK, J. CAVELIER, AND P. JACKSON. 1997. Control of transpiration from the upper canopy of a tropical forest: The role of stomatal, boundary layer and hydraulic architecture components. *Plant Cell Environ.* 20: 1242–1252.
- , ———, ———, ———, ———, AND S. J. WRIGHT. 1999. Partitioning of soil water among canopy trees in a seasonally dry tropical forest. *Oecologia* 121: 293–301.
- MITCHELL, R. J. 1993. Path analysis: Pollination. *In* S. M. Scheiner and J. Gurevitch (Eds.). *Design and analysis of ecological experiments*, pp. 211–231. Chapman and Hall, New York.
- MONCREIFF, J. B., Y. MALHI, AND R. LEUNING. 1996. The propagation of errors in long-term measurements of land-atmosphere fluxes of carbon and water. *Global Change Biol.* 2: 231–240.
- MONTEITH, J. L. 1977. Climate and the efficiency of crop production in Britain. *Philos. Trans. R. Soc. Lond.* 281: 277–294.
- MULKEY, S. S., K. KITAJIMA, AND S. J. WRIGHT. 1996. Plant physiological ecology of tropical forest canopies. *Trends Ecol. Evol.* 11: 408–412.
- , AND S. J. WRIGHT. 1996. Influence of seasonal drought on the carbon balance of tropical forest plants. *In* S. S. Mulkey, R. L. Chazdon, and A. P. Smith (Eds.). *Tropical Forest Ecophysiology*, pp. 187–216. Chapman and Hall, New York.
- MYNENI, R. B., S. O. LOS, AND G. ASRAR. 1995. Potential gross primary productivity of terrestrial vegetation from 1982–1990. *Geophys. Res. Lett.* 22: 2617–2620.
- NICHOL, C. J., K. F. HUEMMERICH, T. A. BLACK, P. G. JARVIS, C. L. WALTHALL, J. GRACE, AND F. G. 2000. Remote sensing of photosynthetic light-use efficiency of boreal forest. *Agric. For. Meteorol.* 101: 131–142.

- PARKER, G. G., A. O. SMITH, AND K. P. HOGAN. 1992. Access to the upper forest canopy with a large tower crane. *BioScience* 42: 664–670.
- PEÑUELAS, J., I. FILELLA, AND J. A. GAMON. 1995. Assessment of photosynthetic radiation-use efficiency with spectral reflectance. *New Phytol.* 131: 291–296.
- , AND Y. INOUE. 2000. Reflectance assessment of canopy CO₂ uptake. *Int. J. Remote Sensing* 21: 3353–3356.
- POTTER, C. S., J. T. RANDERSON, C. B. FIELD, P. A. MATSON, P. M. VITOUSEK, H. A. MOONEY, AND S. A. KLOOSTER. 1994. Terrestrial ecosystem production: A process model based on global satellite and surface data. *Global Biogeochemical Cycles* 7: 811–841.
- PRINCE, S. D., AND S. N. GOWARD. 1995. Global primary production: A remote sensing approach. *J. Biogeogr.* 22: 815–835.
- RAHMAN, A. F., J. A. GAMON, D. A. FUENTES, D. A. ROBERTS, AND D. PRENTISS. 2001. Modeling spatially distributed ecosystem flux of boreal forests using hyperspectral indices from AVIRIS imagery. *J. Geophys. Res.* 106: 33579–33591.
- , V. D. CORDOVA, J. A. GAMON, H. P. SCHMID, AND D. A. SIMS. 2004. Potential of MODIS ocean bands for estimating CO₂ flux from terrestrial vegetation: A novel approach. *Geophys. Res. Lett.* 31: L10503, doi:10.1029/2004GL019778
- RUIMY, A., B. SAUGIER, AND G. DEDIEU. 1994. Methodology for the estimation of terrestrial primary production from remotely sensed data. *J. Geophys. Res.* 99: 5263–5283.
- RUNNING, S. W., AND R. R. NEMANI. 1988. Relating seasonal patterns of the AVHRR vegetation index to simulated photosynthesis and transpiration of forests in different climates. *Remote Sensing Environ.* 24: 347–367.
- RUNYON, J., R. H. WARING, S. N. GOWARD, AND J. M. WELLES. 1994. Environmental limits on net primary production and light-use efficiency across the Oregon Transect. *Ecol. Appl.* 4(2): 226–237.
- SELLERS, P. J. 1985. Canopy reflectance, photosynthesis and transpiration. *Int. J. Remote Sensing* 6: 1335–1372.
- , F. HALL, H. MARGOLIS, B. KELLY, D. BALDOCCHI, G. den HARTOG, J. CIHLAR, M. G. RYAN, B. GOODISON, P. CRILL, J. RANSON, D. LETTENMAIER, AND D. E. WICKLAND. 1995. The Boreal Ecosystem-Atmosphere Study (BOREAS): An overview and early results from the 1994 field year. *Bull. Am. Meteorol. Soc.* 76(9): 1549–1577.
- , F. G. HALL, R. D. KELLY, A. BLACK, D. BALDOCCHI, J. BERRY, M. RYAN, K. J. RANSON, P. M. CRILL, D. P. LETTENMAIER, H. MARGOLIS, J. CIHLAR, J. NEWCOMER, D. FITZJARRALD, P. G. JARVIS, S. T. GOWER, D. HALLIWELL, D. WILLIAMS, B. GOODISON, D. E. WICKLAND, AND F. E. GUERTIN. 1997. BOREAS in 1997: Experiment overview, scientific results, and future directions. *J. Geophys. Res.* 102: 28731–28769.
- , L. BOUNOUA, G. J. COLLATZ, D. A. RANDALL, D. A. DAZLICH, S. O. LOS, J. A. BERRY, I. FUNG, C. J. TUCKER, C. B. FIELD, AND T. G. JENSEN. 1996a. Comparison of radiative and physiological effects of doubled atmospheric CO₂ on climate. *Science* 271: 1402–1406.
- , S. O. LOS, C. J. TUCKER, C. O. JUSTICE, D. A. DAZLICH, G. J. COLLATZ, AND D. A. RANDALL. 1996b. A revised land surface parameterization (SiB2) for atmospheric GCMs. Part II: The generation of global fields of terrestrial biophysical parameters from satellite data. *J. Clim.* 9: 706–737.
- SERRANO, L., J. A. GAMON, AND J. PEÑUELAS. 2000. Estimation of canopy photosynthetic and non-photosynthetic components from spectral transmittance. *Ecology* 81: 3149–3162.
- SHIPLEY, B. 2000. Cause and correlation in biology. A user's guide to path analysis, structural equations and causal inference. Cambridge University Press, Cambridge.
- SHUKLA, J., C. NOBRE, AND P. SELLERS. 1990. Amazon deforestation and climate change. *Science* 247: 1322–1325.
- SOKAL, R. R., AND F. J. ROHLF. 1981. *Biometry*, 2nd Ed. W.H. Freeman & Co., San Francisco.
- STYLINSKI, C. D., J. A. GAMON, AND W. C. OECHEL. 2002. Seasonal patterns of reflectance indices, carotenoid pigments and photosynthesis of evergreen chaparral species. *Oecologia* 131: 366–374.
- TENHUNEN, J. D., F. M. CATARINO, O. L. LANGE, AND W. C. OECHEL (Eds.). 1987. *Plant Responses to Stress: Functional Analysis in Mediterranean Ecosystems*. Springer-Verlag, Berlin.
- TUCKER, C. J., I. Y. FUNG, C. D. KEELING, AND R. H. GAMMON. 1986. Relationship between atmospheric CO₂ variations and a satellite-derived vegetation index. *Nature* 319: 195–199.
- VALENTINI, R., G. MATTEUCCI, A. J. DOLMAN, E.-D. SCHULZE, C. REBMAN, E. J. MOORS, A. GRANIER, P. GROSS, N. O. JENSEN, K. PILEGAARD, A. LINDROTH, A. GRELE, C. BERNHOFER, T. GRÜNWARD, M. AUBINET, R. CEULEMANS, A. S. KOWALSKI, T. VESALA, Ü. RANNIK, P. BERBIGIER, D. LOSTAU, J. GUDMONDSSON, H. THORGEIRSSON, A. IBROM, K. MORGENSTERN, R. CLEMENT, J. MONCREIFF, L. MONTAGNANI, S. MINERBI, AND P. J. JARVIS. 2000. Respiration as the main determinant of carbon balance in European forests. *Nature* 404: 861–865.
- WHITTAKER, R. H. 1975. *Communities and Ecosystems*, 2nd Ed. MacMillan, New York.
- WRIGHT, S. J. 1996. Phenological responses to seasonality in tropical forest plants. *In* S. S. Mulkey, R. L. Chazdon, and A. P. Smith (Eds.). *Tropical Forest Ecophysiology*, pp. 440–469. Chapman and Hall, New York.

APPENDIX

The results of the individual multiple regression analyses summarized in Fig. 6. All variables are nontransformed simple terms, except for Time² included as a predictor of PPF_D. The R² value (= coefficient of multiple determination) that follows each equation indicates the proportion of the variance in the dependent variable explained by the combination of the variables. In the case of a multiple regression, the coefficient for the direct path that links two variables in Fig. 6 is the standard partial regression coefficient (= partial regression coefficient shown in the appropriate equation below divided by the ratio of the standard deviation of the two variables; Sokal and Rohlf, 1981). In the case of a simple regression (*e.g.*, for VP), the path coefficient in Fig. 6 equals a Pearson's product-moment correlation coefficient whose squared value is R². All predictive variables are highly significant ($P < 0.0003$, with partial regression coefficients indicated in bold), except for A_{\max} for *Luehea*'s regression for A ($P = 0.95$).

SPECIAL SECTION

560 Gamon, Kitajima, Mulkey, Serrano, and Wright

Anacardium sp:

$$A = 0.308 A_{\max} + 0.0148 g_s + 0.00251 \text{PPFD} - 1.096 \quad (R^2 = 0.40)$$

$$g_s = 0.0474 \text{PPFD} - 16.6 T_L + 18.2 \text{VP} + 237.2 \quad (R^2 = 0.56)$$

$$T_L = 0.511 \text{Time} + 0.00297 \text{PPFD} + 23.7 \quad (R^2 = 0.48)$$

$$\text{PPFD} = 417.1 \text{Time} - 16.45 \text{Time}^2 - 2020.8 \quad (R^2 = 0.09)$$

$$\text{VP} = -0.2946 \text{Time} + 26.21 \quad (R^2 = 0.26).$$

Luebea sp.:

$$A = 0.00446 A_{\max} + 0.0126 g_s + 0.00951 \text{PPFD} + 0.480 \quad (R^2 = 0.77)$$

$$g_s = 0.254 \text{PPFD} - 38.1 T_L + 43.12 \text{VP} + 401.1 \quad (R^2 = 0.50)$$

$$T_L = 0.483 \text{Time} + 0.00457 \text{PPFD} + 21.8 \quad (R^2 = 0.67)$$

$$\text{PPFD} = 591.8 \text{Time} - 23.54 \text{Time}^2 - 3003.46 \quad (R^2 = 0.21)$$

$$\text{VP} = -0.3126 \text{Time} + 26.03 \quad (R^2 = 0.21)$$